## Title

The relationships between patellofemoral bone remodeling, cartilage composition, and vertical loading rate: PET/MRI in isolated patellofemoral osteoarthritis.



## Journal

Osteoarthritis and Cartilage, 32(12)

## Authors

Bhattacharjee, Rupsa
Hammond, Eric
Chotigar, Ngarmsrikam
et al.

## Publication Date

2024-12-01

## DOI

10.1016/j.joca.2024.09.001

Peer reviewed

Published in final edited form as:

*Osteoarthritis Cartilage*. 2024 December ; 32(12): 1591–1600. doi:10.1016/j.joca.2024.09.001.

# The relationships between patellofemoral bone remodeling, cartilage composition, and vertical loading rate: PET/MRI in isolated patellofemoral osteoarthritis

**Rupsa Bhattacharjee**[#,*], **Eric Hammond**[†], **Ngarmsrikam Chotigar**[#], **Zehra Akkaya**[#,‡], **Fei Jiang**[§], **Emma Bahroos**[#], **Misung Han**[#], **Spencer Behr**[#], **Matthew D. Bucknor**[#], **Richard B. Souza**[#,†], **Valentina Pedoia**[#], **Sharmila Majumdar**[#]

[#]Department of Radiology & Biomedical Imaging, University of California, San Francisco, CA, USA

[†]Department of Physical Therapy and Rehabilitation Science, University of California San Francisco, San Francisco, CA, USA

[‡]Ankara University Faculty of Medicine Radiology Department, Ankara, Turkey

[§]Department of Epidemiology and Biostatistics, University of California San Francisco, San Francisco, CA, USA

## SUMMARY

**Objective:** Loading is invariably an important factor of consideration for understanding the causality flow and parallel existence of articular cartilage and subchondral bone changes. The goal of this study was to investigate the patterns of subregional $^{18}$NaF-SUV vs. $T_{1\rho}$-$T_2$ associations and vertical ground reaction force loading rates; in isolated patellofemoral-joint-osteoarthritis (PFJ-OA) patients.

**Method:** Thirty-five isolated PFJ-OA patients, with no tibiofemoral involvement, underwent simultaneous scans in a 3.0T whole-body hybrid positron emission tomography–magnetic resonance imaging scanner. MRI Whole-Organ Magnetic Resonance Imaging Scoring assessments were performed to identify/confirm isolated PFJ-OA knees from bilateral scans. $T_{1\rho}$-$T_2$ relaxation and SUV values were automatically computed for both trochlear and patellar cartilage and subchondral bone subregions (deep, superficial, lateral, and medial). Maximum vertical impact loading rates (Loading-$Rate_{Norm}$) were calculated from walking trials. Relationships were



[*]Correspondence to: Center of Intelligent Imaging ($CI^2$), Department of Radiology & Biomedical Imaging, University of California, San Francisco (UCSF), QB3 Building, Byers Hall, 2nd Floor, Suite BH-201, 1700 – 4th Street, San Francisco, CA 94158, USA. Rupsa.Bhattacharjee@ucsf.edu (R. Bhattacharjee).

Author contributions

Conception and design: RB, RBS, VP, SM. Acquisition of imaging and biomechanical data: RB, MH, EB, EH, SB. Recruitment of study subjects: RB, MDB. Analysis and interpretation of data: RB, EH, NC, ZA, FJ. Drafting of the article: all authors. Critical revision of the article for important intellectual content: all authors. Final approval of the article: all authors. Guarantor of the integrity of the study: RB.

Conflict of interest

The authors declare no competing interests.

Appendix A. Supporting information

Supplementary data associated with this article can be found in the online version at doi:10.1016/j.joca.2024.09.001.

explored between SUV uptake, $T_{1\rho}$-$T_2$ values, and Loading-$Rate_{Norm}$ via linear mixed-effects modeling.

**Results:** Significant and complex association patterns were noted between medial and lateral bone $^{18}$NaF-SUV uptakes vs. medial and lateral cartilage sub-regional $T_{1\rho}$ and $T_2$. $SUV_{Mean}$ and $SUV_{Max}$ were positively associated with deep cartilage subregional $T_{1\rho}$ *and* $T_2$ values; and negatively associated with superficial cartilage subregional $T_{1\rho}$-$T_2$ values in both medial and lateral regions. Both medial and lateral bone $^{18}$NaF-$SUV_{Mean}$ and $SUV_{Max}$ uptakes remained positively associated with the individual gait characteristics, i.e., peak vertical impact loading rates (Loading-$Rate_{Norm}$).

**Conclusion:** Evidence of simultaneous, complementary, cross-sectional associations between $T_{1\rho}$-$T_2$ values and peak vertical loading rates with $^{18}$NaF-SUV, have been rare in the isolated PFJ-OA cohort. The clinical implications of such novel associations remain of utmost importance from a gait retraining perspective.

### Keywords

Osteoarthritis; Patello-femoral; PET/MRI; Sodium-fluoride; Loading-Rate; Gait

## Introduction

Knee osteoarthritis (OA), being a common cause of physical disability, pain, and degradation in quality of life, has a significant fiscal impact.[1,2] Imaging studies involving radiographs and magnetic resonance imaging (MRI) reveal approximately 64% of adults over the age of 50 suffer from patellofemoral joint (PFJ) OA, and one-third of them have isolated PFJ-OA.[3] Isolated radiographic PFJ-OA is a more common occurrence than isolated tibiofemoral joint (TFJ)-OA, and several studies[4–6] have reported mixed-OA to likely start as symptomatic isolated PFJ-OA. Interestingly, depending on variations of risk factors, occurrences of PFJ cartilage damage can remain stable as well as isolated, and might not propagate to the other compartments in some instances.[7] Therefore, a better understanding of the intricate processes in isolated PFJ-OA leading to treatment and prevention strategies specifically targeting the PFJ is warranted.

Having scar tissues formed on cartilage does not necessarily manifest as OA unless special conditions accelerate the process.[5] Increased bone remodeling in the early stage of cartilage damage could be one such acceleration condition, aided by bi-directional bone-cartilage crosstalk, cellular signaling, and vascular invasions. Evidence of bone-cartilage crosstalk and parallel existence of bone remodeling as well as cartilage degenerations, has been well explored via morphological, metabolic, and compositional MRI.[8,9] Initial degradation of cartilage indicated by an increase in water content, proteoglycan loss, and disruption of the collagen network[8] can be quantitatively evaluated by $T_{1\rho}$ and $T_2$ relaxation time mapping on MRI.[8] Standardized uptake values (SUV) from Sodium Fluoride ($^{18}$NaF) positron emission tomography (PET) imaging,[10] on the other hand, is a well-documented marker for quantifying ongoing bone remodeling by the actions of bone-resorbing osteoclasts and bone-forming osteoblasts,[9] and rapid metabolic bone response to load.[11] These imaging

tools have, however, been explored majorly in isolation, and rarely in the context of isolated PFJ-OA.

While investigating bone-cartilage crosstalk, loading is invariably an important factor of consideration for understanding the causality flow and parallel existence of articular cartilage and subchondral bone changes. Moderate mechanical loading is generally documented to cause hypertrophy,[12] thereby accelerating proteoglycan loss and collagen disruption, causing significant changes in $T_{1\rho}$ and $T_2$ relaxation times. Although the initiation point of the causal flow remains unclear, the existence of a cyclic positive feedback loop between cartilage compositional change, damage of mechanical integrity, and increased bone remodeling thereafter to enable the joint to adapt to the altered loads, is well established. Literature has shown ample evidence of increased $T_{1\rho}$ and $T_2$ relaxation time associations with increased shear loading and decreased relaxation time correlations with increased compressive forces and pressures.[13,14] The findings hint towards the cartilage composition of OA subjects having a reduced capability to dissipate loads, in general. A complex pathophysiological crosstalk between compositional and metabolic processes and its association with loading is hypothesized, beyond just parallel independent co-existence.

Very little is known about the biomechanical loading factors associated with isolated PFJ-OA in particular, and how those factors might be associated with the inter-imaging relationships via MRI.[15] Abnormal patellofemoral loading during activities of daily living often is a major contributor to pain and symptoms in the joint.[13,16] Understanding loading profiles in combination with comprehensive patellofemoral imaging is seemingly essential to designing therapeutic interventions, therefore.[17,18] Vertical ground reaction forces (vGRF) and moments are usually common forms of measurement to understand the individualistic knee loading characteristics.[14] Associations between knee joint loading rate and joint degeneration have previously been reported in animal and cadaveric studies.[19] Strong associations between knee joint loading rate during walking and OA have been studied in humans as well, not explicitly evaluated for isolated PFJ-OA though.[19] Recent advances in gait retraining methods provide new opportunities for biomechanical breakthroughs in the treatment of OA.[20,21] Since most biomechanical features are potentially modifiable, they offer promises for developing disease-modifying treatment strategies.

We hypothesized that elevated SUV in subjects with isolated PFJ-OA might be colocalized with the prolongation of $T_{1\rho}$ and $T_2$ relaxation times. Additionally, complex bone-cartilage interactions could also be associated with loading rates as a result of abnormal gait biomechanics. Therefore, this study aimed to investigate the patterns of subregional (medial and lateral, deep, and superficial) associations between (a) trochlear and patellar bone $^{18}$NaF-SUV values, (b) cartilage $T_{1\rho}$ and $T_2$ characteristics, and (c) vGRF loading rates in individuals having isolated PFJ-OA, via statistical modeling.

## Materials and methods

### Subjects

In this ongoing prospective study, approved by the local Institutional Review Board, the subjects were identified from the clinical database of all the patients referred for a clinical

knee MRI examination by the Orthopedic and Sports Medicine clinics and care-plan services on campus. A radiologist (MB, 14 years of expertise in musculoskeletal imaging), assessed the MRI images and reports of all potential subjects from the pre-existing clinical knee MRI scans. Study inclusion was confirmed if the subjects had cartilage lesions or definite osteophytes on patellar and/or trochlear compartments in either or both knees. Potential subjects with MRI evidence of TFJ involvement or tri-compartmental osteophytes were excluded. The following set of inclusion criteria was applied: a) being skeletally mature (aged 28–80 years), b) being within a Body-Mass-Index (BMI) cutoff (< =37 $kg/m^2$) or a knee circumference < =49 cm (due to physical constraint of MRI flex coil); since High BMI is well known to negatively affect the data quality of both motion analysis and MR imaging, c) experiencing pain in stair ascent and/or descent, and d) having a prior clinical MRI scan for primary assessment. Subjects with a history of traumatic knee involvement, tendon and ligament injuries or tears, complex meniscus tears, patellar tendinosis, rheumatoid arthritis, or contact injury at the knee, having vestibular conditions affecting gait mechanics, having contradictions to MRI, being injected with corticosteroid within the past six weeks, or having used investigational drugs, were excluded from the study. Subjects who fulfilled the required criteria underwent simultaneous $^{18}$NaF-PET/MRI imaging and motion analysis data (within 4 days of the MRI Scan) collection from December 2021 to November 2023 for inclusion in this study. Written informed consent was provided by the subjects before data collection. No formal sample size calculation was performed given the proof-of-concept nature of this study.

## PET-MRI acquisition

All participants underwent MRI scan acquisitions in a 3.0T whole-body hybrid PET-MRI scanner (Signa PET-MR, GE Healthcare, Waukesha, WI, USA) capable of simultaneous acquisition of both time-of-flight (TOF) PET and high-resolution MRI acquisition.[6] The subjects were positioned supine, feet-first. Two 16-channel medium flex receive-only coils (NeoCoil, Pewaukee, WI, USA) were wrapped around each knee for bilateral knee acquisitions. Shims and center frequencies were automatically calculated based on left and right shim volumes, for ensuring uniform fat suppression on simultaneous bilateral knee acquisitions. For MRI, bilateral sagittal three-dimensional (3D) proton-density fat-saturated fast-spin-echo (3D PDFS FSE i.e., Cube, whole joint) and bilateral axial magnetization-prepared angle-modulated partitioned k-space spoiled gradient echo snapshots (MAPSS, dedicated for PFJ) sequences[22] were acquired for both knees for morphological and compositional (combined $T_{1\rho}$ and $T_2$) assessments, respectively. For simultaneous PET, $^{18}$F-NaF was used as a PET tracer, sourced from the institutional cyclotron facility, and produced using current good manufacturing practices guidelines.[23] Based on preliminary studies,[6] an average dose of 294.87 ± 59.78 (range 191.20 – 370) MBq of [$^{18}$F]-NaF was injected intravenous to each patient. Average radiotracer uptake was 60-minute per patient. Therefore, the 20-minute static-PET scan was started at the 60-minute mark, after injection. An effective dose of 0.024 mSv/MBq was used to calculate the radiation exposure to each subject due to the injected [$^{18}$F]-NaF. PET images were reconstructed by a TOF Ordered Subsets-Expectation Maximization algorithm. Dixon fat-water MR images were used for MR-based attenuation correction of PET photons.[24] The detailed protocol is summarized in Table I.

### MRI analysis

The stepwise pipeline for image processing and analysis is demonstrated in Fig. 1. Bilateral knee sagittal Cube, axial MAPSS (first-echo images, computed $T_{1\rho}$, $T_2$ maps), $^{18}$NaF-PET images, and SUV maps were geometrically resampled and co-registered with the sagittal Cube images. Medial and lateral patella and trochlea subchondral bone masks were generated. The patellar and trochlear cartilages were automatically and separately subdivided into four regions: deep-medial (DM), deep-lateral (DL), superficial-medial (SM), and superficial-lateral (SL). The mean $T_{1\rho}$ and $T_2$ relaxation values for four sub-regions ($T_{1\rho}$-DM, $T_{1\rho}$-SM, $T_{1\rho}$-DL, $T_{1\rho}$-SL, $T_2$-DM, $T_2$-SM, $T_2$-DL, and $T_2$-SL in ms), were computed separately for both PFJ (patella and trochlear) cartilages. Similarly, mean and max SUV values for two PFJ bony subregions ($SUV_{Mean}$-medial, $SUV_{Mean}$-lateral, $SUV_{Max}$-medial, $SUV_{Max}$-lateral), both trochlear and patellar, were automatically and separately computed. In the final imaging analysis data structure: the two subchondral bone SUV values (medial, lateral) and four subregional cartilage $T_{1\rho}$ and $T_2$ values (DM, SM, DL, SL), were recorded and paired under the same tissue tag (patellar/trochlear), PFJOA-knee-laterality tag (right/left), and subject ID. A detailed image processing description of the above methods has been provided in the Supplementary Materials.

### Motion analysis data

All testing was performed at the institution's Human Performance Center. Following a static standing calibration trial, all subjects performed a series of walking trials across two in-ground force plates along a 10–m walkway at 1.35 m/s. Participants completed a minimum of five successful walking trials for each leg. A successful trial was defined as a trial in which the entire foot strike fell entirely within one force plate. GRF data were recorded at 1000 Hz from two in-ground AMTI force platforms (AMTI, Watertown, MA 02472)[25–27] and were low-pass filtered (Butterworth 4th order, phase lag, 50 Hz, based on residual frequency analysis) using Visual3D (C-Motion, Germantown, MD). The vGRF magnitude data were then normalized for patient mass (N/Kg).[26] During the fixed walk, the average (instantaneous) slope of each trial was calculated from 20–80% of the vGRF magnitude at the first peak. Finally, the maximum vertical impact loading rates ($Loading\text{-}Rate_{Norm}$) were calculated[27] from all average (instantaneous) slopes over all the trials (N/kg/s).

### Statistical analysis

Descriptive statistics were used to describe the characteristics of each demographic, compositional, metabolic, and gait characteristics for the PFJ-OA knees. Continuous variables were tested for normality using the Shapiro-Wilk test. Log transformations for age, $SUV_{Mean}$-medial, $SUV_{Mean}$-lateral, $SUV_{Max}$-medial, $SUV_{Max}$-lateral, and $Loading\text{-}Rate_{Norm}$ were made to meet model assumptions of normality; other model assumptions were reasonable.

To explore the associations between bone remodeling, cartilage compositional characteristics, and peak vertical impact loading rates ($Loading\text{-}Rate_{Norm}$), eight linear mixed-effects models (LMEs) were built between SUV measures (outcomes) and $T_{1\rho}$ and $T_2$ measures (predictors) in PFJ-OA knees, using maximum-likelihood, independent residual errors, and Nelder-Mead optimizer, to obtain the parameter estimators.[28]

Four medial models were: Model-1: $SUV_{Mean}$-medial vs. $T_{1\rho}$-DM + $T_{1\rho}$-SM + Loading-$Rate_{Norm}$, Model-2: $SUV_{Max}$-medial vs. $T_{1\rho}$-DM + $T_{1\rho}$-SM + Loading-$Rate_{Norm}$, Model-3: $SUV_{Mean}$-medial vs. $T_2$-DM + $T_2$-SM + Loading-$Rate_{Norm}$, Model-4: $SUV_{Max}$-medial vs. $T_2$-DM + $T_2$-SM + Loading-$Rate_{Norm}$. Four were lateral models: Model-5: $SUV_{Mean}$-lateral vs. $T_{1\rho}$-DL + $T_{1\rho}$-SL + Loading-$Rate_{Norm}$, Model-6: $SUV_{Max}$-lateral vs. $T_{1\rho}$-DL + $T_{1\rho}$-SL + Loading-$Rate_{Norm}$, Model-7: $SUV_{Mean}$-lateral vs. $T_2$-DL + $T_2$-SL + Loading-$Rate_{Norm}$, Model-8: $SUV_{Max}$-lateral vs. $T_2$-DL + $T_2$-SL + Loading-$Rate_{Norm}$. The medial models included medial, bone-cartilage paired data for both tissue types (patellar and trochlear). Similarly, the lateral models included lateral, bone-cartilage paired data for both tissue types (patellar and trochlear). Multiple (patellar and trochlear, medial and lateral) subregions were extracted from each knee. A single subject could potentially have occurrences of PFJ-OA in both knees. Therefore, we include nested random effects which assume data from the same Knee-Laterality and from the same subject, share the same random components. 1| Knee-Laterality/Patient-ID was used as nested random effects in the LMEs, with Knee-Laterality and the person as level 1 and 2 grouping variables. These were Random intercept models. The covariance structure was independent. The residuals of the eight models met model assumptions of linearity and variance, were normally distributed, and posterior predictive checks were assessed. 95% Confidence Intervals (CIs) and p-values were obtained from the Wald test. All analyses were conducted using ‘rcompanion’, ‘flexplot’, lme4′, and ‘medsense’ packages in RStudio (version 12.0+353; https://www.r-project.org/), using $p < 0.05$ to determine statistical significance.

## Results

### Participant characteristics

A total of thirty-five subjects (18 females and 17 males, mean age: 49.02 ± 12.61 years, BMI: 26.12 ± 4.48 kg/$m^2$) fulfilled all criteria and were recruited in the study. Based on the Whole-Organ Magnetic Resonance Imaging Scoring (WORMS) assessment,[29] thirty-eight knees were identified as isolated PFJ-OA (three female subjects had bilateral isolated PFJ-OA). The descriptive details are summarized in Table II.

### Associations between bone remodeling and cartilage compositional characteristics

Performances of the eight LME models are summarized in Tables III and IV. After adjusting for within-subject and within-knee clustering, metabolic activities ($SUV_{Mean}$ and $SUV_{Max}$) remained positively associated with deep cartilage subregional $T_{1\rho}$ *and* $T_2$ values; and negatively associated with superficial cartilage subregional $T_{1\rho}$ *and* $T_2$ values over all the medial and lateral LME models. The strengths of associations were noted in terms of beta estimates, 95% CIs, and p-values (Tables III and IV). The strengths of associations of $SUV_{Mean}$ and $SUV_{Max}$ with subregional $T_{1\rho}$ values (both in medial Model-1 vs. Model-2; and lateral Model-5 vs. Model-6) were very similar (beta estimates, 95% CIs). Similarly, the strengths of associations of $SUV_{Mean}$ and $SUV_{Max}$ with subregional $T_2$ values (both in medial Model-3 vs. Model-4 and lateral Model-7 vs. Model-8) were very close.

Similarly, performances of models having $T_{1\rho}$ values as predictors and $T_2$ values as predictors (medial models 1 vs. 3, 2 vs. 4; lateral models 5 vs. 7, 6 vs. 8) were very similar

(beta estimates, and 95% CIs) as well. The similarities point to the higher collinearities between $SUV_{Mean}$ and $SUV_{Max}$ values (outcomes) as well as between $T_{1\rho}$ *and* $T_2$ values (predictors). Demonstrative $T_{1\rho}$, $T_2$, and SUV images of two subjects are visualized in Fig. 2.

### Associations between bone remodeling and gait characteristics

As summarized in Tables III and IV, After adjusting for within-subject and within-knee clustering, metabolic activities ($SUV_{Mean}$ and $SUV_{Max}$) remained positively associated with peak vertical impact loading rates ($Loading\text{-}Rate_{Norm}$) over all the medial and lateral LME models. The strengths of associations were noted in terms of beta estimates, 95% CIs, and p-values (Tables III and IV). The strengths of associations of $SUV_{Mean}$ and $SUV_{Max}$ with $Loading\text{-}Rate_{Norm}$ (both in medial Model-1 vs. Model-2; and lateral Model-5 vs. Model-6) were very similar (beta estimates, 95% CIs). The similarities point to the higher collinearities between $SUV_{Mean}$ and $SUV_{Max}$ values (outcomes). Demonstrative maximum vertical impact loading rates ($Loading\text{-}Rate_{Norm}$) of two subjects over multiple trials are shown in Fig. 3.

## Discussion

In the simultaneous PET/MRI study of patients having isolated PFJ-OA, significant and complex association patterns were noted between medial and lateral bone $^{18}$NaF-SUV uptakes vs. medial and lateral cartilage sub-regional $T_{1\rho}$ and $T_2$ values in trochlear and patellar regions. The deep cartilage associations were positive whereas the superficial cartilage ones were negative. Both medial and lateral bone $^{18}$NaF-SUV uptakes were positively associated with the individual gait characteristics, i.e., maximum vertical impact loading rates.

The current study design enables examination of the cross-sectional relationships between cartilage biochemistry, quantified using compositional quantitative MRI techniques, and bone turnover (metabolism) assessed using SUV from an $^{18}$NaF PET tracer. This study was also, one of the first, to explore the association of gait biomechanics in these interactions. A pre-existing MRI-based selection of PFJ-OA cohort before recruitment and a WORMS scoring afterward,[30] ensured that the study findings were solely focused on understanding PFJ-OA-specific associations. The specified demographics represent the most susceptible population to OA. Additionally, the high resolution of the axial 3D MAPSS ensured efficient $T_{1\rho}$ and $T_2$ quantification with reduced partial volume effects as much as possible.

One of the striking findings of the current study was how compositional relaxation parameters of deep cartilage were associated positively with $^{18}$NaF uptake, while the superficial regions were associated negatively (Tables III and IV). The trend remains the same for both lateral and medial models, irrespective of selections of predictors ($T_{1\rho}$ and $T_2$) and outcomes ($SUV_{Mean}$ and $SUV_{Max}$). It hints towards almost two complementary mechanisms working in parallel at the cartilage level; collagen-breakdown or proteoglycan-loss in the deep cartilage layer accelerating the bone-remodeling, and simultaneously the superficial layer being preserved. The superficial layer of the cartilage can be speculated to have a varied degree of fluid permeability in the collagen matrix than the deeper layer.

It could happen either to preserve the integrity via transporting the water content of the cartilage to the deeper layer or to compensate for it. Similar instances of contrastive mechanisms and depth-dependent biochemical variations have previously been reported in the superficial and deep layers of the femoral cartilage in response to loading in healthy and OA groups.[31] Evidence of morphological variations, i.e., simultaneous thinning and thickening of different regions of the same cartilage exists on large-scale longitudinal data as well.[32] Mosher et.al has reported significant reductions in $T_2$ times of the superficial femoral cartilage post-dynamic loading.[33] In post-traumatic OA development following anterior cruciate ligament reconstruction surgery, similar but opposite evidence of two complementary mechanisms working in parallel has been reported, which is aided more commonly by superficial degeneration than deeper cartilage.[34] Hinted in multiple unique instances, complementary balance mechanisms might be an intrinsic pathophysiological way of maintaining a state of homeostasis and preventing rapid widespread cartilage degeneration. However, there are no concrete proofs of these speculative theories. Whether there are plausible biological reasons behind it, related to inflammation, or could it be a mechanical way of counter-balancing the load distribution in the joint; remains to be investigated.

The selection of SUV values as an outcome and $T_2$ (or $T_{1\rho}$) values as exposures in the mediation analysis, as well as in the LME, could raise obvious questions and one might suggest interchangeable directionality. Technically, given the nature of PET acquisition and the lower resolution of images compared to MRI, uptake measurements are limited to and averaged over comparatively larger regions. The range of variability in SUV values is smaller as well, to capture heterogeneity at a smaller scale of voxels. On the contrary, using isotropic higher resolution axial MAPSS focused to scan just the PFJ region, improves confidence on reduced partial volume effects in $T_2$ (and $T_{1\rho}$) values, and the range of measurements is much larger for characterizing small variations in the otherwise homogenous patient cohort. From a pathophysiological perspective, the positive feedback loop of cartilage collagen-matrix breakdown (prolongation in $T_2$ values), cartilage-bone crosstalk, and bone remodeling (increase in 18 NaF-SUV uptake) is reported to be cyclic rather than unidirectional. With the current study design, we cannot claim the initiation of causal phenomenon happens at the level of cartilage and then mediated via biomechanical loading behaviors to the bone, with confidence. However, the certainty of the causal flow of effects from cartilage to bone mediated via an individualistic loading pattern holds at some level of the whole feedback loop.

The strong connection between loading mechanics on the PFJ and the disease of the joint has been extensively reported in the literature. The positive association between the rates of change in patellofemoral loading and patellofemoral pain has been documented by Atkins et.al.[26] Subjects with patellofemoral pain often tend to adapt compensatory strategies to reduce flexion, adopting a “stiff-legged gait”, which alters the lower extremity absorption mechanisms and increases vGRF loading rates. The aberrant lower extremity mechanics, including altered vGRFs, and load increase, in turn, are reported to aggravate patellofemoral pain, producing mechanical and biochemical changes in the environment of the knee.[35] Viscoelastic joint tissues respond to loading in a time-dependent manner, i.e., degenerative diseases have a positive association with higher rates of loading.[35] In subjects with TFJ OA,

independent relationships exist between knee adduction moment loading rate (measured at the medial compartment of the TFJ) and medial TFJ degeneration.[19] Evidence of simultaneous association/relationships in $T_2$ (and $T_{1\rho}$) values, $^{18}$NaF-SUV uptake, and peak vertical loading rates, have been rare, especially in an isolated PFJ-OA cohort. Therefore, the clinical implications of such associations remain of utmost importance from a gait retraining perspective for lowering vertical impact loading rates.[36]

Having established evidence of cross-sectional associations, longitudinal studies in the future can help understand whether peak vertical loading rates act as a mediation factor between bone-cartilage crosstalk. If so, could gait interventional design help lowering loading rates, and arrest the progression of degenerative changes in PFJ-OA? The causal mediation analysis in the future would also raise questions on to what extent the lateral and medial aspects of the degenerations are driven mechanically, and systemically accounting for relevant confounders. The current study is limited in its ability to answer those questions.

## Limitations

Walking, although not often a common problem associated with pain in subjects with isolated PFJ-OA, is the most common activity performed easily by most individuals. Novel interventions focused on gait modification often identify peak vertical impact loading rates (during walking) as the primary variable of interest.[37] However, other biomechanical characteristics (such as knee extensor moment impulse, peak knee abduction moment, or peak trunk flexion angle), as well as data collected from sit-to-stand and rising from a chair are available for this cohort. and have been excluded for the sake of avoiding collinearity and simplifying the analysis, otherwise complex already. These will be included in future studies focused on biomechanical multivariate analysis in PFJ-OA. Additionally, male and female subjects could have inherent differences in the compositional-metabolic-gait manifestation of PFJ-OA. By achieving a higher sex-ratio balance with the inclusion of more subjects in this ongoing study, a stratified subgroup analysis would be possible. Similarly, in the current study, even with separate trochlear and patellar data, the overall patellofemoral regional associations and model conclusions were generalized from a medial vs. lateral perspective. Considering the $T_{1\rho}$ and $T_2$ relaxation values in patellar regions will vary from the trochlear regions, due to orientation dependence and the magic angle effects, a higher sample size and subsequent sub-group analysis for trochlear and patellar perspectives would be crucial. The imaging metrics computed in this study, $T_{1\rho}$ and $T_2$ as well as semi-quantitative SUV often suffer from natural variations amongst patients and might not be ideal to use in a cross-sectional study setting as absolute measures. Significant associations irrespective of the natural variances hint at a potential underestimation of true association patterns. Re-examining the relative associations in longitudinal studies would therefore be the most conclusive choice. Finally, the study was limited in the number of patients. There has been a lack of reported studies investigating isolated PFJ-OA cartilage-bone PET/MRI and gait associations. Therefore, the estimation of a prior sample size was difficult. We believe the significant observations and standardized effects reported in this study can further be utilized as a validation tool for sample size estimation. Further studies are warranted to overcome these limitations.

## Conclusion

In this bilateral PET/MRI study of isolated PFJ-OA subjects, bone remodeling markers ($SUV_{Mean}$ and $SUV_{Max}$) were positively associated with deep cartilage subregional $T_{1\rho}$ *and* $T_2$ values; and negatively associated with superficial cartilage subregional $T_{1\rho}$ *and* $T_2$ values in trochlear and patellar, medial, and lateral regions. In both lateral and medial PFJ subregions, positive associations were noted between bone SUV values and normalized maximum ground reaction force loading rates.

## Supplementary Material

Refer to Web version on PubMed Central for supplementary material.

## Role of funding sources

This study was funded by the National Institutes of Health (NIH-NIAMS) grant R01AR079647.

## References

1. Lawrence RC, Felson DT, Helmick CG, et al. Estimates of the prevalence of arthritis and other rheumatic conditions in the United States. Part II. Arthritis Rheum 2008;58:26–35. [PubMed: 18163497]
2. Guccione AA, Felson DT, Anderson JJ, et al. The effects of specific medical conditions on the functional limitations of elders in the Framingham Study. Am J Public Health 1994;84:351–8. [PubMed: 8129049]
3. Duncan R, Peat G, Thomas E, Wood L, Hay E, Croft P. Does isolated patellofemoral osteoarthritis matter? Osteoarthritis Cartilage 2009;17:1151–5. [PubMed: 19401244]
4. Duncan R, Peat G, Thomas E, Hay EM, Croft P. Incidence, progression and sequence of development of radiographic knee osteoarthritis in a symptomatic population. Ann Rheum Dis 2011;70:1944–8. [PubMed: 21810840]
5. Burr DB, Gallant MA. Bone remodelling in osteoarthritis. Nat Rev Rheumatol 2012;8:665–73. [PubMed: 22868925]
6. Tibrewala R, Pedoia V, Bucknor M, Majumdar S. Principal component analysis of simultaneous PET-MRI reveals patterns of bone–cartilage interactions in osteoarthritis. J Magn Reson Imaging 2020;52:1462–74. [PubMed: 32207870]
7. Stefanik JJ, Guermazi A, Roemer FW, et al. Changes in patellofemoral and tibiofemoral joint cartilage damage and bone marrow lesions over 7 years: the Multicenter Osteoarthritis Study. Osteoarthritis Cartilage 2016;24:1160–6. [PubMed: 26836287]
8. Gallo MC, Wyatt C, Pedoia V, et al. T1ρ and T2 relaxation times are associated with progression of hip osteoarthritis. Osteoarthritis Cartilage 2016;24:1399–407. [PubMed: 26973330]
9. Park PSU, Raynor WY, Sun Y, Werner TJ, Rajapakse CS, Alavi A. 18F-sodium fluoride PET as a diagnostic modality for metabolic, autoimmune, and osteogenic bone disorders: cellular mechanisms and clinical applications. Int J Mol Sci 2021;22:6504. [PubMed: 34204387]
10. Kogan F, Fan AP, McWalter EJ, Oei EHG, Quon A, Gold GE. PET/MRI of metabolic activity in osteoarthritis: a feasibility study. J Magn Reson Imaging 2017;45:1736–45. [PubMed: 27796082]
11. Watkins LE, Haddock B, MacKay JW, et al. [$^{18}$F]Sodium fluoride PET-MRI detects increased metabolic bone response to whole-joint loading stress in osteoarthritic knees. Osteoarthritis Cartilage 2022;30:1515–25. [PubMed: 36031138]
12. Jørgensen AEM, Kjær M, Heinemeier KM. The effect of aging and mechanical loading on the metabolism of articular cartilage. J Rheumatol 2017;44:410–7. [PubMed: 28250141]

13. Song K, Scattone Silva R, Hullfish TJ, Silbernagel KG, Baxter JR. Patellofemoral joint loading progression across 35 weight-bearing rehabilitation exercises and activities of daily living. Am J Sports Med 2023;51:2110–9. [PubMed: 37272685]
14. Bigouette J, Simon J, Liu K, Docherty CL. Altered vertical ground reaction forces in participants with chronic ankle instability while running. J Athl Train 2016;51:682–7. [PubMed: 27813684]
15. Zhou X, Shen X. MRI semi-quantitative evaluation of clinical features of cartilage injury in patients with osteoarthritis. Concepts Magn Reson Part A 2022;2022:1–10.
16. Van Rossom S, Smith CR, Zevenbergen L, et al. Knee cartilage thickness, T1ρ and T2 relaxation time are related to articular cartilage loading in healthy adults. PLoS One 2017;12, e0170002. [PubMed: 28076431]
17. Tsai Y-J, Powers CM. Increased shoe sole hardness results in compensatory changes in the utilized coefficient of friction during walking. Gait Posture 2009;30:303–6. [PubMed: 19553123]
18. Manal K, McClay I, Stanhope S, Richards J, Galinat B. Comparison of surface mounted markers and attachment methods in estimating tibial rotations during walking: an in vivo study. Gait Posture 2000;11:38–45. [PubMed: 10664484]
19. Morgenroth DC, Medverd JR, Seyedali M, Czerniecki JM. The relationship between knee joint loading rate during walking and degenerative changes on magnetic resonance imaging. Clin Biomech 2014;29:664–70.
20. Roper JL, Harding EM, Doerfler D, et al. The effects of gait retraining in runners with patellofemoral pain: a randomized trial. Clin Biomech 2016;35:14–22.
21. Davis IS, Tenforde AS, Neal BS, Roper JL, Willy RW. Gait retraining as an intervention for patellofemoral pain. Curr Rev Musculoskelet Med 2020;13:103–14. [PubMed: 32170556]
22. Li X, Han ET, Busse RF, Majumdar S. In vivo T(1rho) mapping in cartilage using 3D magnetization-prepared angle-modulated partitioned k-space spoiled gradient echo snapshots (3D MAPSS). Magn Reson Med 2008;59:298–307. [PubMed: 18228578]
23. Hung JC. Bringing new PET drugs to clinical practice – a regulatory perspective. Theranostics 2013;3:885–93. [PubMed: 24312157]
24. Chen Y, An H. Attenuation correction of PET/MR imaging. Magn Reson Imaging Clin N Am 2017;25:245–55. [PubMed: 28390526]
25. Tsai Y-J, Powers CM. The influence of footwear sole hardness on slip characteristics and slip-induced falls in young adults. J Forensic Sci 2013;58:46–50. [PubMed: 23062013]
26. Atkins LT, James CR, Yang HS, et al. Changes in patellofemoral pain resulting from repetitive impact landings are associated with the magnitude and rate of patellofemoral joint loading. Clin Biomech 2018;53:31–6.
27. Schmida EA, Wille CM, Stiffler-Joachim MR, Kliethermes SA, Heiderscheit BC. Vertical loading rate is not associated with running injury, regardless of calculation method. Med Sci Sports Exerc 2022;54:1382–8. [PubMed: 35320147]
28. Nelder JA, Mead R. A simplex method for function minimization. Comput J 1965;7:308–13.
29. Peterfy CG, Guermazi A, Zaim S, et al. Whole-organ magnetic resonance imaging score (WORMS) of the knee in osteoarthritis. Osteoarthritis Cartilage 2004;12:177–90. [PubMed: 14972335]
30. Hunter DJ, Arden N, Conaghan PG, et al. Definition of osteoarthritis on MRI: results of a Delphi exercise. Osteoarthritis Cartilage 2011;19:963–9. [PubMed: 21620986]
31. Souza RB, Kumar D, Calixto N, et al. Response of knee cartilage T1rho and T2 relaxation times to in vivo mechanical loading in individuals with and without knee osteoarthritis. Osteoarthritis Cartilage 2014;22:1367–76. [PubMed: 24792208]
32. Cummings J, Gao K, Chen V, et al. The knee connectome: a novel tool for studying spatiotemporal change in cartilage thickness. J Orthop Res 2024;42:43–53. [PubMed: 37254620]
33. Mosher TJ, Smith HE, Collins C, et al. Change in knee cartilage T2 at MR imaging after running: a feasibility study. Radiology 2005;234:245–9. [PubMed: 15550376]
34. Wang L-J, Zeng N, Yan Z-P, Li J-T, Ni G-X. Post-traumatic osteoarthritis following ACL injury. Arthritis Res Ther 2020;22:57. [PubMed: 32209130]

35. Briani RV, Pazzinatto MF, Waiteman MC, de Oliveira Silva D, de Azevedo FM. Association between increase in vertical ground reaction force loading rate and pain level in women with patellofemoral pain after a patellofemoral joint loading protocol. Knee 2018;25:398–405. [PubMed: 29655902]

36. Crowell HP, Davis IS. Gait retraining to reduce lower extremity loading in runners. Clin Biomech 2011;26:78–83.

37. Corrigan P, Davis IS, James KA, Crossley KM, Stefanik JJ. Reducing knee pain and loading with a gait retraining program for individuals with knee osteoarthritis: protocol for a randomized feasibility trial. Osteoarthr Cartil Open 2020;2, 100097. [PubMed: 36474880]

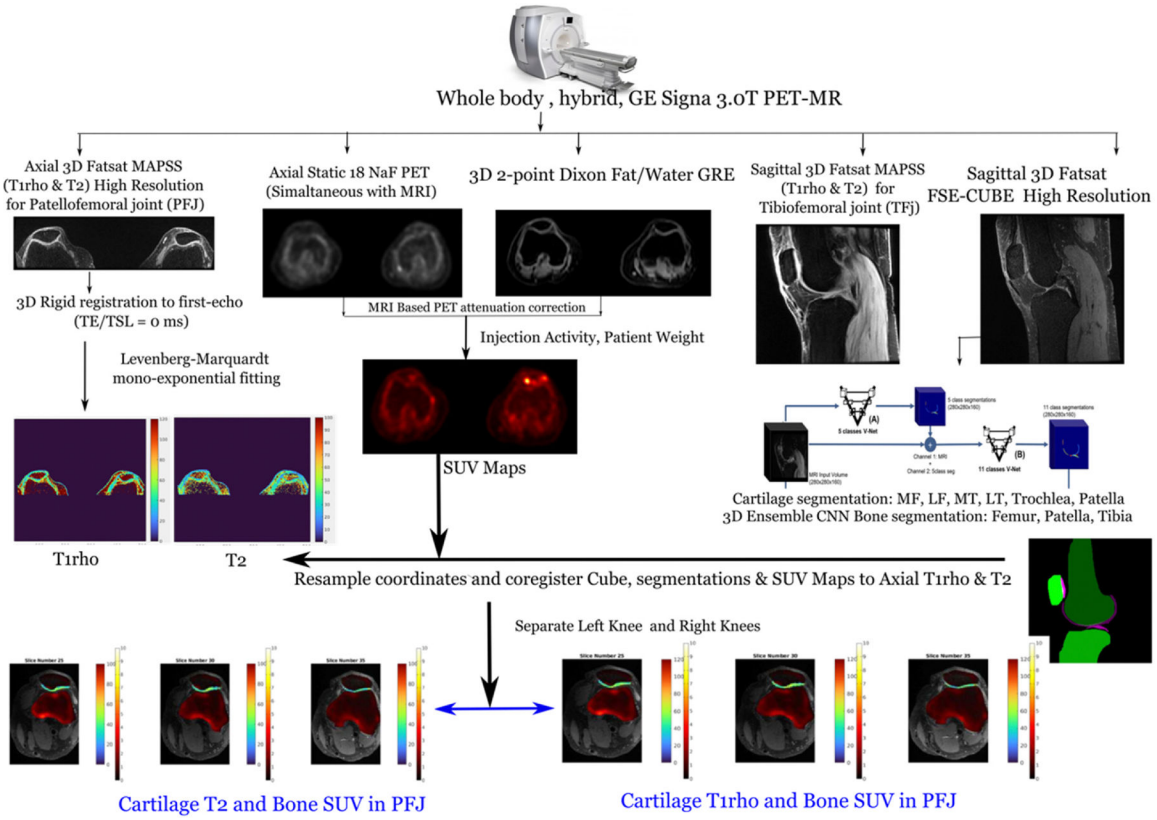


**Fig. 1.**

Schema of Methodology: Image acquisition, processing, segmentation, analysis, and evaluation.

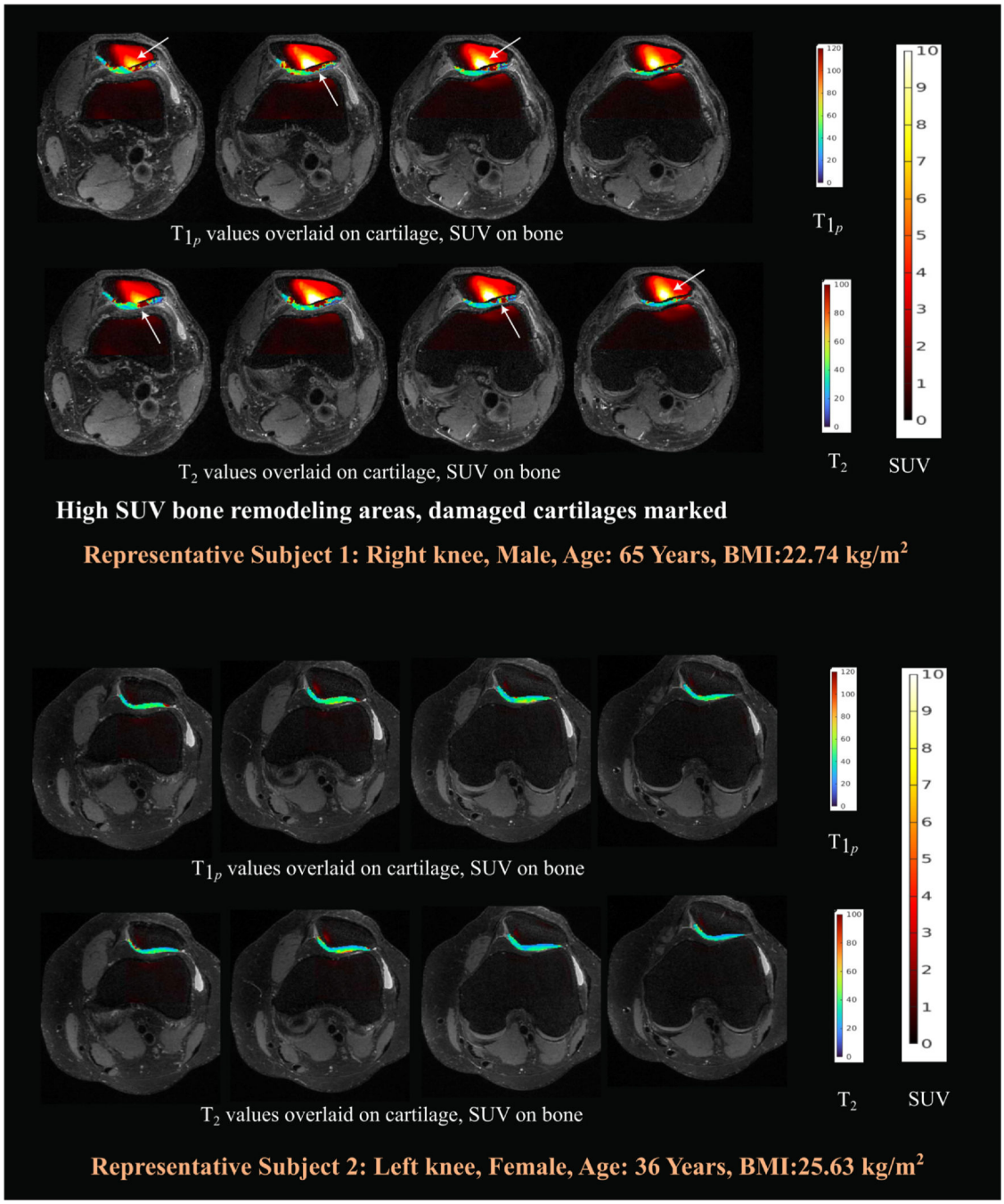


**Fig. 2.**

Demonstrative $T_{1\rho}$, $T_2$, and SUV images of two subjects. Subject 1: Right knee of a Male (65 years aged) subject with isolated PFJ-OA. Subject 2: Left knee of a Female (36 years aged) subject with isolated PFJ-OA.

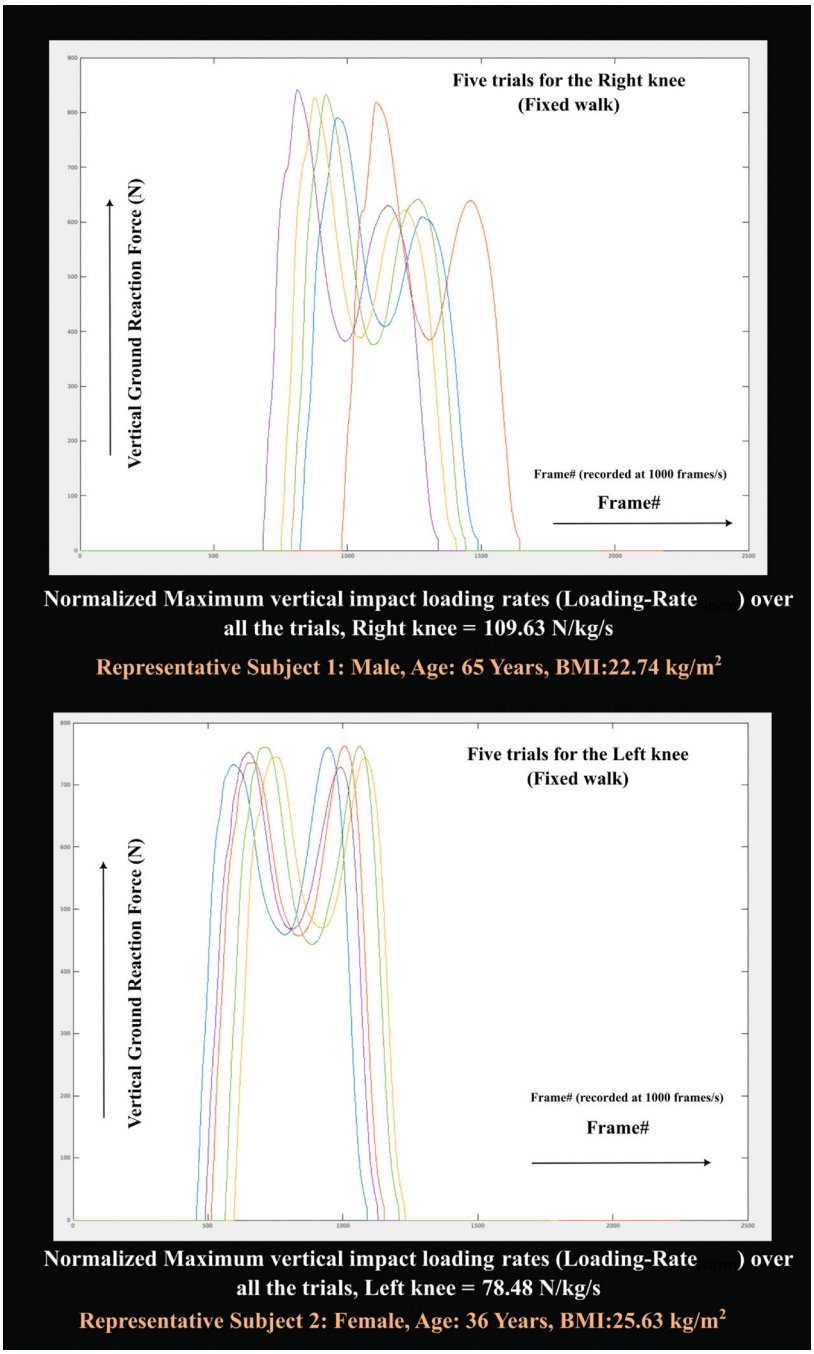


**Fig. 3.**

Demonstrative maximum vertical impact loading rates (Loading-Rate$_{Norm}$) of two subjects over multiple trials. Subject 1: Right knee of a Male (65 years aged) subject with isolated PFJ-OA. Subject 2: Left knee of a Female (36 years aged) subject with isolated PFJ-OA.

**Table I**

Acquisition parameters for simultaneous PET-MRI sequences utilized in this study.

| Imaging Sequences | | Scan Parameters | Resolution/Scan Time | Assessment |
|---|---|---|---|---|
| Sagittal Prescription | 3D fat-sat FSE-Cube | FOV= 15 × 15 $cm^2$; 256 × 256 matrix size; 0.6 mm slice thickness; 600 slices; TR/TE= 1200/26 ms; BW= ±62.5 kHz; ETL = 32; ARC AF ($k_y \times k_z$) = 2 × 3 | Isotropic 0.6 mm/13 mins | Overall morphological assessment of the whole joint, for isolated PFJ-OA confirmation |
| | 3D fat-sat $T_{1\rho}$ and $T_2$ MAPSS | FOV = 14 × 14 $cm^2$; 256 × 128 matrix size; 4 mm slice thickness; 78 slices; TR/TE = 8.4/2.1 ms; BW= ±62.5 kHz; $T_{rec}$= 1.2 s; 64 views per preparation; TSL= 0/10/40/80 ms; FSL= 500 Hz; TE for $T_2$-preparation = 0/12.8/25.7/51.4 ms; ARC AF ($k_y \times k_z$) = 2 × 3 | 0.55 × 1.1 × 4 $mm^3$/12 mins | $T_{1\rho}$ and $T_2$ quantification of TFJ cartilage (**Not Used in this study**) |
| Axial Prescription | 3D fat-sat $T_{1\rho}$ and $T_2$ MAPSS | FOV = 5.76 × 29.2 $cm^2$; 64 × 324 matrix size; 64 slices; 0.9 mm slice thickness; TR/TE = 4.5/2.1 ms; BW= ±31.25 kHz; $T_{rec}$= 1.2 s; 128 views per preparation; TSL= 0/10/40/80 ms; FSL= 500 Hz; TE for $T_2$-preparation = 0/12.8/25.7/51.4 ms; ARC AF ($k_y \times k_z$) = 3 × 1 | Isotropic 0.9 mm/ 23 mins | $T_{1\rho}$ and $T_2$ quantification of PFJ cartilage |
| | 3D 2-point Dixon Fat/Water GRE | FOV = 40 × 30 $cm^2$; 256 × 96 matrix size; 64 slices; 5 mm slice thickness; TR = 4 ms; 2 TEs; BW= ±83.3 kHz | 1.56 × 3.13 × 5 $mm^3$/ 20 s | For MR-based PET attenuation correction |
| | Static PET (Simultaneous with MRI scanning 60 min) | Transverse Filter Cutoff 3 mm, Subset 28, Iterations/Axial Filter 4/Standard | 1.95 × 1.95 × 2.78 $m^3$ | SUV bone remodeling |

FSE = Fast-Spin-Echo, FOV = Field of View, TE = Echo time, TR = Repetition time, BW = Bandwidth, ETL = Echo Train Length, ARC = Auto calibrating Reconstruction for Cartesian imaging, MAPSS = Magnetization-Prepared Angle-Modulated Partitioned k-Space Spoiled Gradient Echo Snapshots, TSL = time of spin lock, PFJ = Patellofemoral Joint, TFJ = Tibiofemoral Joint, GRE = Gradient-Echo, SUV = Standardized Uptake Value.

**Table II**

Demographic, morphological, compositional, metabolic and gait characteristics of the study cohort.

| **Descriptor** | **Isolated PFJ-OA (n = 35 subjects, 38 Knees)** | | | | | | | |
|---|---|---|---|---|---|---|---|---|
| Age (years) | 48.98 ± 12.16 | | | | | | | |
| Sex assigned at Birth | 18 females, 17 males | | | | | | | |
| BMI (kg/m$^2$) | 25.55 ± 4.71 | | | | | | | |
| | Score 0 | Score 1 | Score 2 | Score 2.5 | Score 3 | Score 4 | Score 5 | Score 6 |
| [a]Patellar WORMS$_{Cartilage}$ | 10.81% | 16.21% | 32.43% | 2.70% | 16.21% | 2.70% | 16.21% | 2.70% |
| [a]Trochlear WORMS$_{Cartilage}$ | 48.71% | 25.64% | 15.38% | 0% | 7.69% | 0% | 2.56% | 0% |
| [a]Patellar WORMS$_{BME}$ | 64.86% | 5.40% | 27.02% | NA | 2.70% | NA | NA | NA |
| [a]Trochlear WORMS$_{BME}$ | 89.74% | 0% | 7.69% | NA | 2.56% | NA | NA | NA |
| | **Patella** | | | | **Trochlea** | | | |
| | **Medial** | | **Lateral** | | **Medial** | | **Lateral** | |
| Mean SUV | 0.53 ± 0.39 | | 0.59 ± 0.57 | | 0.68 ± 0.48 | | 0.65 ± 0.41 | |
| Max SUV | 2.24 ± 2.30 | | 2.80 ± 2.68 | | 2.82 ± 2.49 | | 3.05 ± 2.53 | |
| | **Superficial** | **Deep** | **Superficial** | **Deep** | **Superficial** | **Deep** | **Superficial** | **Deep** |
| Mean $T_{1\rho}$ (ms) | 50.85 ± 11.75 | 47.87 ± 13.85 | 51.05 ± 12.14 | 47.99 ± 12.17 | 40.02 ± 10.63 | 41.99 ± 11.02 | 42.81 ± 9.23 | 44.69 ± 7.92 |
| Mean $T_2$ (ms) | 35.56 ± 9.96 | 33.36 ± 11.13 | 36.15 ± 9.84 | 34.07 ± 9.77 | 29.32 ± 8.69 | 30.28 ± 8.84 | 31.42 ± 7.55 | 32.19 ± 6.10 |
| Normalized Max Average Vertical Impact Loading Rate (Loading-Rate$_{Norm}$: N/Kg/s) | 77.72 ± 20.72 | | | | | | | |

Information presented as mean ± standard deviation for continuous variables.

WORMS = whole-organ magnetic resonance imaging scores, SUV = Standardized Uptake Values.

[a]Data expressed as percentage of the total sample.

**Table III**

Summary of linear mixed effects (LME) medial models (including knee-laterality/person-ID) as nested random effects) for the association between bone subregional SUV parameters vs. cartilage subregional $T_{1\rho}$ and $T_2$ values and vertical loading rates.

| Outcome | Predictors | Estimates, β | (95% CI) | p-value | Comments |
|---|---|---|---|---|---|
| LME Medial Models | | | | | |
| Model 1: $SUV_{Mean}$-medial | $T_{1\rho}$-DM | exp (0.05 * 1 unit of $T_{1\rho}$-DM) ~= 1.051% | [1.01–1.083%] | 0.011 * | Model findings are similar |
| | $T_{1\rho}$-SM | exp (−0.06 * 1 unit of $T_{1\rho}$-SM) ~= 0.941% | [0.904–0.98%] | < 0.001 *** | |
| | $Loading\text{-}Rate_{Nom}$ | exp (1.36 * 1 unit of $Loading\text{-}Rate_{Norm}$) ~= 3.89% | [1.363–11.023%] | 0.012 * | |
| Model 2: $SUV_{Max}$-medial | $T_{1\rho}$-DM | exp (0.04* 1 unit of $T_{1\rho}$-DM) ~= 1.04% | [1.003–1.083%] | 0.035 * | |
| | $T_{1\rho}$-SM | exp (−0.06 * 1 unit of $T_{1\rho}$-SM) ~= 0.941% | [0.904–0.98%] | 0.006 ** | |
| | $Loading\text{-}Rate_{Nom}$ | exp (1.51 * 1 unit of $Loading\text{-}Rate_{Norm}$) ~= 4.526% | [1.309–15.486%] | 0.018 ** | |
| Model 3: $SUV_{Mean}$-medial | $T_2$-DM | exp (0.07 * 1 unit of $T_2$-DM) ~= 1.072% | [1.020–1.116%] | 0.004 ** | Model findings are similar |
| | $T_2$-SM | exp (−0.083 * 1 unit of $T_2$-SM) ~= 0.923% | [0.878–0.961%] | 0.001 ** | |
| | $Loading\text{-}Rate_{Nom}$ | exp (1.34 * 1 unit of $Loading\text{-}Rate_{Norm}$) ~= 3.819% | [1.349–10.804%] | 0.012 * | |
| Model 4: $SUV_{Max}$-medial | $T_2$-DM | exp (0.06 * 1 unit of $T_2$-DM) ~= 1.061% | [0.96–1.173%] | 0.233 | |
| | $T_2$-SM | exp (−0.07 * 1 unit of $T_2$-SM) ~= 0.932% | [0.843–1.03%] | 0.166 | |
| | $Loading\text{-}Rate_{Nom}$ | exp (2.29 * 1 unit of $Loading\text{-}Rate_{Norm}$) ~= 9.874% | [1.072–18.835%] | 0.044 * | |

Estimates (β) represent the change in outcome (%) associated with one unit change in the predictors.

Cartilages: DM = Deep-Medial, SM = Superficial-Medial. CI = Confidence Interval.

Significance Codes = 0 '***' 0.001 '**' 0.01 '*' 0.05 '.' 0.1 ' ' 1.

**Table IV**

Summary of linear mixed effects (LME) lateral models (including knee-laterality/person-ID) as nested random effects) for the association between bone subregional SUV parameters vs. cartilage subregional $T_{1\rho}$ and $T_2$ values and vertical loading rates.

| Outcome | Predictors | Estimates, β | (95% CI) | p-value | Comments |
|---|---|---|---|---|---|
| LME Lateral Models | | | | | |
| Model 1: $SUV_{Mean}$-lateral | $T_{1\rho}$-DL | exp (0.06 * 1 unit of $T_{1\rho}$-DL) ~= 1.061% | [1.03–1.094%] | < 0.001 *** | Model findings are similar |
| | $T_{1\rho}$-SL | exp (−0.06 * 1 unit of $Tt_p$-SL) ~= 0.941% | [0.913–0.97%] | < 0.001 *** | |
| | $Loading\text{-}Rate_{Norm}$ | exp (1.34 * 1 unit of $Loading\text{-}Rate_{Norm}$) ~= 3.819% | [1.336–10.913%] | 0.013 * | |
| Model 2: $SUV_{Max}$-lateral | $T_{1\rho}$-DL | exp (0.05 * 1 unit of $T_{1\rho}$-DL) ~= 1.051% | [1.01–1.094%] | 0.013 * | |
| | $T_{1\rho}$-SL | exp (−0.04 * 1 unit of $T_{1\rho}$-SL) ~= 0.96% | [0.932–0.996%] | 0.029 ** | |
| | $Loading\text{-}Rate_{Norm}$ | exp (1.40 * 1 unit of $Loading\text{-}Rate_{Norm}$) ~= 4.055% | [1.233–13.463%] | 0.022 * | |
| Model 3: $SUV_{Mean}$-lateral | $T_2$-DL | exp (0.08 * 1 unit of $T_2$-DL) ~= 1.083% | [1.03–1.127%] | < 0.001 *** | Model findings are similar |
| | $T_2$-SL | exp (−0.07 * 1 unit of $T_2$-SL) ~= 0.932% | [0.895–0.97%] | < 0.001 *** | |
| | $Loading\text{-}Rate_{Norm}$ | exp (1.15 * 1 unit of $Loading\text{-}Rate_{Norm}$) ~= 3.158% | [1.116–8.935%] | 0.03 * | |
| Model 4: $SUV_{Max}$-lateral | $T_2$-DL | exp (0.06 * 1 unit of $T_2$-DL) ~= 1.061% | [1.009–1.116%] | 0.019 * | |
| | $T_2$-SL | exp (−0.04 * 1 unit of $T_2$-SL) ~= 0.96% | [0.923–1.001%] | 0.06 | |
| | $Loading\text{-}Rate_{Norm}$ | exp (1.3 * 1 unit of $Loading\text{-}Rate_{Norm}$) ~= 3.669% | [1.105–12.061%] | 0.034 * | |

Estimates (β) represent the change in outcome (%) associated with one unit change in the predictors.

Cartilages: DL = Deep-Lateral, SL = Superficial-Lateral. CI = Confidence Interval.

Significance Codes = 0 '*** ' 0.001 '**' 0.01 '*' 0.05 '.' 0.1 ' ' 1.